J. Biochem. 131, 437–444 (2002)

# Effect of Antifungal Azoles on the Heme Detoxification System of Malarial Parasite

**Nguyen Tien Huy, Kaeko Kamei,[1] Yoshiro Kondo, Satoshi Serada, Kenji Kanaori, Ryo Takano, Kunihiko Tajima, and Saburo Hara**

*From the Department of Applied Biology, Kyoto Institute of Technology, Matsugasaki, Sakyo-ku, Kyoto 606-8585*

Received December 18, 2001; accepted December 27, 2001

**The antimalarial activities of some antifungal azole agents (ketoconazole, miconazole, and clotrimazole) have been known for several years, however, their antimalarial mechanism remains equivocal. Our recent study showed that clotrimazole has a relative high affinity for heme, inhibits reduced glutathione-dependent heme catabolism, and enhances heme-induced hemolysis. In the present study, we have found that clotrimazole can remove heme from histidine rich peptide-heme complex, which initiates heme-polymerization in malaria. In addition, we show that two other azoles (ketoconazole and miconazole) behave similarly to clotrimazole in binding to heme: they bind to heme with similar affinities, remove heme from the histidine rich peptide-heme complex and from the reduced glutathione-heme complex to form stable heme-azole complexes with two nitrogenous ligands derived from the imidazole moieties of two azole molecules. We have also revealed that clotrimazole and miconazole have stronger promoting activities for heme-induced hemolysis than ketoconazole, implying that the stronger antimalarial activities of clotrimazole and miconazole might arise from their stronger ability to promote heme-induced hemolysis of clotrimazole and clotrimazole than that of ketoconazole. These results also suggest that ketoconazole and miconazole, like clotrimazole, might possess an antimalarial mechanism relating to their inhibition of heme polymerization and the degradation of reduced glutathione-dependent heme.**

**Key words: antifungal azoles, antimalarial, ESR, heme, malaria.**

Malaria is one of the most common diseases in tropic countries. Each year, there are 300 million new malarial infections along with millions of deaths all over the world. The control and treatment of malaria are difficult due to several factors including the resistance of mosquitoes to insecticides and the resistance of parasites to antimalarial drugs (*1*). Thus, there is an urgent need for new effective antimalarials to cure malarial patients.

Since malaria degrades hemoglobin as a major source of amino acids during its intra-erythrocytic stage, free heme is released inside the malarial compartment. The released heme, which is extremely hazardous to the cell membrane, changes the homeostasis of the malarial cell, binds to some malarial enzymes and inhibits their activities causing malaria death (*2–5*). To protect itself, the malaria parasite develops several possible protective mechanisms to detoxify free heme released during hemoglobin catabolism. Some of the free heme (30–50%) is subsequently polymerized to non-toxic hemozoin in the food vacuole through the formation of a complex with *Plasmodium falciparum* histidine-rich protein 2 (PfHRP2), which is made up repeats of three amino acids: histidine (34%), alanine (37%), and aspartic acid (10%) (*6, 7*). The remaining non-polymerized free heme passes through the membrane of food vacuoles and reaches the cytosol of the parasite (*8–11*). In the cytosol, reduced glutathione (GSH) binds to heme via its thiol and degrades heme (*12, 13*). In binding to heme, GSH competes with the membrane (*14*) since hydrophobic compounds such as heme have an affinity for the membrane. However, millimolar GSH in the malarial cytoplasm (*15, 16*) is enough to bind heme despite the low affinity ($K_D = 2.8 \times 10^{-3}$ M). This indicates that GSH could protect malaria from toxic heme released from hemoglobin. In spite of the existence of these protective mechanisms, free heme is still found in malaria-infected red blood cells, parasite compartments, parasite food vacuoles (*17*) and associated with cell membranes (*8, 14, 18*). However, due to the balance between the release of free heme from hemoglobin and the detoxification of heme by malaria, the concentrations of free heme in malaria parasites and red blood cells are so low that malaria can multiply. Thus, this need to keep the concentration of free heme low, which is both unique to the parasite and vital to its survival, is an ideal target for developing an antimalarial drug.

Previous studies have demonstrated that antifungal azoles, ketoconazole (Keto), miconazole (Mico), and clotrimazole (CLT), effectively and rapidly inhibit the growth of

[1] To whom correspondence should be addressed. Tel: +81-75-724-7553, Fax: +81-75-724-7532, E-mail: kame@ipc.kit.ac.jp

Abbreviations: CLT, clotrimazole; DMSO, dimethyl sulfoxide; EDT, 1,2-ethanedithiol; ESR, electron spin resonance; Fmoc, 9-fluorenylmethyloxycarbonyl; GSH, reduced glutathione; HEPES, 2-[4-(2-hydroxyethyl)-1-piperazinyl]ethanesulfonic acid; HOBt, 1-hydroxybenzotriazole; Keto, ketoconazole; Mico, miconazole; PfHRP2, *Plasmodium falciparum* histidine rich protein 2; t-Bu, *tert*-butyl; TBS, Tris buffer saline (20 mM Tris-HCl, pH 7.4, containing 0.9 % NaCl); TFA, trifluoroacetic acid; Trt, trytyl. We defined ferric protoporphyrin IX as heme or protoheme, and ferric mesoprotoporphyrin IX as mesoheme.

© 2002 by The Japanese Biochemical Society.



Downloaded from http://jb.oxfordjournals.org/ at Islamic Azad University on September 29, 2012

chloroquine-resistant strains of *P. falciparum in vitro* (*19–23*). As shown in Fig. 1, the three azoles share the structural feature of possessing an imidazole group.

The effect of CLT on calcium ion flux has been proposed as the primary mechanism of the antimalarial activity of CLT (*23–26*). We have recently shown that CLT has a high binding affinity for ferric heme to form a heme-CLT complex assuming the ferric low-spin state (S = 1/2) with two nitrogenous ligands derived from the imidazole moieties of two CLT molecules (*13*). The formation of the heme-CLT complex disturbs heme degradation by GSH, and the complex damages the cell membrane more seriously than free heme does (*13*). Therefore, another antimalarial mechanism of CLT might be the disruption of the protective system of malaria against free heme. In this work, we studied further the effect of Keto and Mico as well as CLT on PfHRP2-dependent heme catabolism using a peptide based on the repetitive sequence of PfHRP2 (Ala-His-His-Ala-His-His-Ala-Ala-Asp) and found that all three azoles can remove heme from the histidine-rich peptide-heme complex. We have also revealed that CLT and Mico have stronger promoting activities of heme-induced hemolysis than Keto. In addition, using optical absorption and ESR spectroscopy, we studied the binding affinities of Keto and Mico to heme and their inhibitory activities against GSH-dependent heme catabolism.

## MATERIALS AND METHODS

*Materials*—GSH, CLT, Mico, and hemin (heme) were purchased from Sigma. Human blood was from healthy volunteers. Dimethyl sulfoxide (DMSO) was from Wako, Tokyo. Fmoc-amino acids were obtained from Peptide Institute (Osaka). Mesoheme was from Porphyrin Products (USA) and Keto was from ICN Biomedicals (USA). All other chemicals were of the highest available grade.

*Peptide Synthesis*—The model peptide R27 was synthesized according to the repetitive amino acid sequence of PfHRP2 as follows: Ala-His-His-Ala-His-His-Ala-Ala-Asp-Ala-His-His-Ala-His-His-Ala-Ala-Asp-Ala-His-His-Ala-His-His-Ala-Ala-Asp (Three repetitive units of Ala-His-His-Ala-His-His-Ala-Ala-Asp).

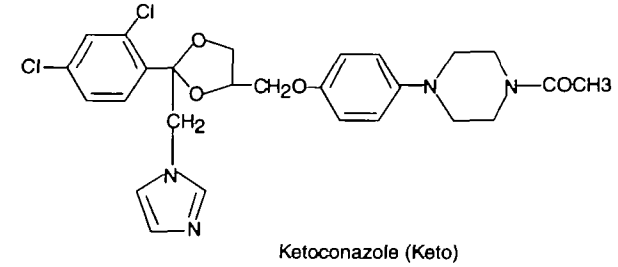


Ketoconazole (Keto)

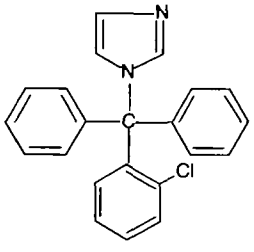


Clotrimazole (CLT)

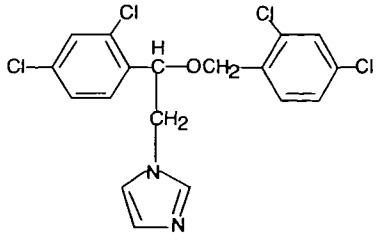


Miconazole (Mico)

Fig. 1. **Chemical structures of azoles.**

The peptide was synthesized by a solid-phase procedure using TGS-PHB-Asp(t-Bu)-resin and Fmoc-amino acids on an automatic peptide synthesizer (model PSSM-8, Shimadzu, Kyoto). All deblocking, rinsing, and coupling steps were carried out according to the manufacturer's manual. Temporary protection of the side chains of His and Asp was accomplished with Trt and t-Bu groups, respectively. Couplings were performed with HOBt active esters. After synthesis, the peptide was cleaved from the resin with 94% TFA containing 5% anisole and 1% EDT at room temperature for 2 h. The peptide was recovered as a precipitate with diethyl ether.

The synthesized peptide was purified by reverse phase chromatography using an Inertsil ODS-3 (4.6 × 250 mm, GL Science) column on a high performance liquid chromatograph (HPLC). The column was equilibrated with 0.1% TFA and eluted with an 80-min linear gradient from 0 to 80% acetonitrile containing 0.1% TFA. The flow rate was 1 ml/min and the eluate was monitored by the absorbance at 230 nm. The peptide was obtained as a single peak by repetitive chromatographies under the same conditions described above.

The molecular mass of the purified peptide was determined in a positive mode by a laser ionization TOF mass spectrometer (Kratos Analytical, KOMPACT MALDI II, Manchester, UK). The amino acid composition and peptide concentration were determined using an amino acid analyzer (Hitachi, model L-8500A, Tokyo) after hydrolysis with 6 N HCl at 110°C for 24 h *in vacuo*. The results of mass spectrometry and amino acid analysis of the peptide were identical to the expected results.

*Hemin Preparation*—A fresh stock heme solution was prepared by dissolving hemin chloride in 20 mM NaOH, then centrifuging for 10 min at 15,000 rpm to remove the remaining hemin crystals. Heme concentrations were estimated from the absorbance at 385 nm using $\varepsilon_{mM}$ = 58,400 in 100 mM NaOH (*27*), and adjusted to 1 mM by diluting with 20 mM NaOH. This stock solution (1 mM) was kept in the dark on ice and used within 24 h.

*Absorption Spectra*—All absorption spectra were recorded on a Hitachi U-3300 double beam spectrophotometer (Tokyo) using 1.0-cm lightpath quartz cuvettes at 25°C. The conditions of measurement are described in the figure legends.

*Spectrometric Titration*—Differential absorption spectra were also measured on a Hitachi U-3300 double beam spectrophotometer as described in a previous report (*13*). Briefly, the binding of azoles to heme was titrated by adding increasing amounts of azoles into the sample cuvette containing 10 μM heme in 20 mM HEPES buffer (pH 7.4) containing 40% DMSO, and into the first reference cuvette containing the same solution without heme. The second reference cuvette contained 10 μM heme in 20 mM HEPES buffer (pH 7.4) containing 40% DMSO but not contained azoles. We confirmed that the pH of the solution did not change when heme solution was added under these conditions. In the present study, we used the increase in the Soret band absorbance at 416 nm to monitor the formation

Downloaded from http://jb.oxfordjournals.org/ at Islamic Azad University on September 29, 2012

of heme-Keto complexes, while the heme-Mico complex was evaluated based on the Soret band absorbance at 424 nm.

The binding of azoles to heme may be represented by the equilibrium as follows:

$$H + nD \longleftrightarrow H(D)_n \quad (1)$$

and the association affinity constant of the heme-azole complex was determined from the Hill plot (*28, 29*):

$$\log\frac{A - A_0}{A_x - A} = -\log K_D + n \log[D] \quad (2)$$

Where D, azole; H, heme; $H(D)_n$, heme-azole complex; $K_D$, dissociation affinity constant of the heme-azole complex; [D], azole concentration; $A_0$, the absorbance of heme in the absence of added azole; $A$, the absorbance of the mixture of heme and azole at an azole concentration of [D]; $A_x$, the absorbance of the mixture of heme and azole when no further absorption intensity increased indicating that all heme had formed the complex with azoles.

*ESR Measurement of Heme-Keto and Heme-Mico Complexes*—For ESR measurements, we used mesoheme instead of heme (protoheme) because mesoheme is more stable at high concentration. Heme-Keto and heme-Mico complexes (0.5 mM mesoheme and 2.5 mM azoles) were prepared in DMSO. After incubation for 1 h at room temperature, the ESR spectra of the complexes were recorded by a JES-TE 300 ESR Spectrometer (Tokyo) at 4.2 K with 100 kHz field modulation. The frequency counter in the spectrometer monitored the microwave frequency of each measurement. The magnetic field strength was calibrated by hyperfine splitting of Mn(II) ion (8.69 mT) doped in MgO powder. Powdered lithium-tetracyano-quinodimethane radical (Li-TCNQ, $g$ = 2.0025) was used as the standard for $g$-values. The ESR data were analyzed and calibrated using a Winrad system (Radical Research, Tokyo). The typical conditions for ESR measurement were as follows: microwave power, 6.0 mW; modulation magnitude, 0.68 mT; sweep range 30 mT to 500 mT; sweep time, 4 min; and time constants, 0.1 s.

*Effect of Keto, CLT, and Mico on the Heme-R27 Complex*—The heme-R27 complex (0.5 mM mesoheme and 0.5 mM R27) was prepared in 100 mM phosphate buffer containing 2.86% DMSO (pH 7.4). After incubation for 1 h at room temperature, the ESR spectrum of the complex was recorded with the same ESR spectrometer under the conditions described above. Then, 60 mM azoles in DMSO were sequentially added into the solution containing the heme-R27 complex to make a final azole concentration in the range of 0.5–4 mM in 0.5 mM increments. The sample was mixed and incubated for 15 min at room temperature. In this experiment, the DMSO concentration ranged from 2.86–5%, since at this range of concentration, DMSO has no influence on the ESR spectrum of the heme-R27 complex. At the end of incubation, the spectrum was recorded again at 4.2 K using the ESR spectrometer to observe the effect of azoles on the heme-R27 complex.

*Inhibition of GSH-Dependent Heme Degradation by Keto and Mico*—Heme degradation by GSH was monitored by measuring the absorbance at 396 nm as described in our previous study (*13*). Heme (3 μM) and GSH (2 mM) were mixed in HEPES buffer (200 mM, pH 7.4) in the presence or absence of Keto (6 μM) or Mico (6 μM), and then the absorbance at 396 nm was continuously recorded for 30 min at 37°C.

*Azole Concentrations That Cause 50% Erythrocyte Hemolysis ($EC_{50}$) in the Presence of 5 μM Heme*—Blood from healthy volunteers was heparinized (1 mg heparin/ml of blood) to prevent clotting. The erythrocytes were separated from the plasma by centrifugation at 1,500 ×$g$ for 3 min and washed six times with TBS. Thereafter, the effects of azoles on heme-dependent hemolysis were studied with 0.5% cell suspensions in TBS. Suspensions of 0.5 % erythrocytes (0.6 ml) were shaken at 140 cycles/min with 5 μM heme in the presence of various concentrations of azoles. After incubation at 37°C for 150 min, the sample was centrifuged to remove the non-hemolyzed erythrocytes. The amount of hemoglobin released from the hemolyzed erythrocytes into the supernatant was determined from the absorbance at 578 nm (*13*). Then the hemoglobin content in the non-hemolyzed erythrocytes collected as a pellet was measured from the absorbance at 578 nm after lysis with distilled water and centrifugation. The ratio of hemoglobin content released from the hemolyzed erythrocytes to that of total erythrocytes was expressed as a percentage and assumed to represent the extent of hemolysis by 5 μM heme. The concentration of azoles that caused 50% erythrocyte hemolysis ($EC_{50}$) in the presence of 5 μM heme was calculated on the basis of the semi-logarithmic concentration-response curve using a GraphPad Prism (USA).

## RESULTS

*Absorption Spectra of Heme in Complex with Keto and Mico*—The absorption spectrum of heme (12 μM) in phosphate buffer (pH 7.4) shows Soret band absorption at 342 and 385 nm, and Q band absorption at 493 and 613 nm, representing the mixture of the monomer and the aggregated form of heme with five coordinate structures (*30–32*) with a weak axial ligand such as water, oxygen, or chloride anion. By adding 40 μM Keto and Mico, the Soret bands underwent a red-shift to 414 and 417 nm, respectively, and Q band absorptions were evident at 534 and 562 nm for both the heme-Keto and heme-Mico complexes as shown in Fig. 2 and Table I. Neither azole shows absorption in the range from 300 to 700 nm (data not shown). These observed spectra indicate that both the heme-Keto and heme-Mico complexes may assume a six coordinate structure. Typical spectra of six coordinate structures indicate that aggregated heme also dissociates into monomers and forms complexes with Keto or Mico. In addition, other heme-bis-imidazole complexes (*33, 34*), including the heme-CLT complex described in our previous study (*13*), as summarized in Table I, gave similar spectra, supporting the concept that Keto and Mico have an affinity for the heme chromophore and suggesting that imidazole groups in these drugs should act as donors for the formation of heme-azole complexes.

*Spectrophotometric Heme Titration with Keto and Mico*—The interactions of heme with Keto and Mico were further studied using spectrophotometric titration experiments as described in "MATERIALS AND METHODS." During the formation of heme-azole complexes, the spectral changes were accompanied by a lowering of the Soret molar absorption and a shift of the Soret band maximum to a longer wavelength (data not shown).

The observed spectral changes were analyzed by Hill plots (*28, 29*) as described in our previous study (*13*) to de-



Downloaded from http://jb.oxfordjournals.org/ at Islamic Azad University on September 29, 2012

termine the number of azole molecules bound to the heme in aqueous DMSO. Since it has been reported that heme in aqueous DMSO (40%) exists as a monomer up to a heme concentration of 26.6 μM (*35–37*), we used a solution containing 40% DMSO to analyze the binding mode of heme and azoles. As shown in Fig. 3, the Hill plots of the binding data of heme and the two azoles (Keto and Mico) indicate that the slopes of the linear graphs are nearly 2. This suggests that the formation of the heme-azole complex proceeds cooperatively at two non-identical binding sites. Furthermore, the results of the Hill plots reveal that heme binds to Keto and Mico with dissociation constants ($K_D$) of $2.8 \times 10^{-9}$ $M^2$ and $1.7 \times 10^{-9}$ $M^2$, respectively, as summarized in Table II. The azole concentrations that are required for half saturation ($SC_{50}$) of 10 μM heme were also estimated from the Hill plots as summarized in Table II.

*ESR Spectra of Heme-Keto and Heme-Mico Complexes*— The electronic and coordination structures of the heme-Keto and heme-Mico complexes were further investigated by ESR. The observed ESR spectrum (Fig. 4a) of mesoheme (0.5 mM) gave a typical line shape ($g = 6$ and $g = 2.0$) of a ferric high-spin (S = 5/2) species, taking five coordination geometry into account (*38*). A weak signal was always observed at about $g = 4.3$, which may be due to non-heme iron from decomposed heme (*39*) or due to impurities in the sample tube and dewar assembly. When Keto or Mico (2.5 mM) was mixed with mesoheme (0.5 mM), the ESR spectra showed line shapes ascribed to ferric low-spin species with $g$ values of $g_1 = 1.46$, $g_2 = 2.26$, and $g_3 = 2.97$ for the heme-Keto complex (Fig. 4b); and $g_1 = 1.49$, $g_2 = 2.26$, and $g_3 = 2.98$ for the heme-Mico complex (Fig. 4c). The observed ESR line widths of these heme-azole complexes were quite similar to those recorded for heme-CLT and heme-imidazole complexes (*13*). In addition, the observed $g$-values of those complexes agreed well with each other (*e.g.*, proto-heme-imidazole and proto heme–cytochrome *b*-559 complexes) (Table III). This provides experimental evidence that both heme-Keto and heme-Mico complexes assume a ferric low-spin state (S = 1/2), with two nitrogenous ligands derived from the imidazole groups of the two azole mole-

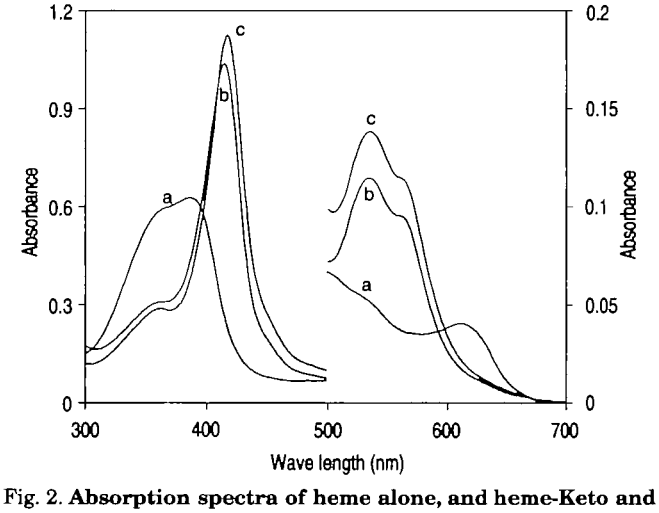


Fig. 2. **Absorption spectra of heme alone, and heme-Keto and heme-Mico complexes.** Absorption spectra were measured in 100 mM phosphate buffer, pH 7.4, after 5-min mixing of heme (12 μM) and azoles (40 μM) when no further spectral changes were observed. a, heme alone; b, heme-Keto complex; c, heme-Mico complex. Left *y*-axis, Soret region; right *y*-axis, Q region.

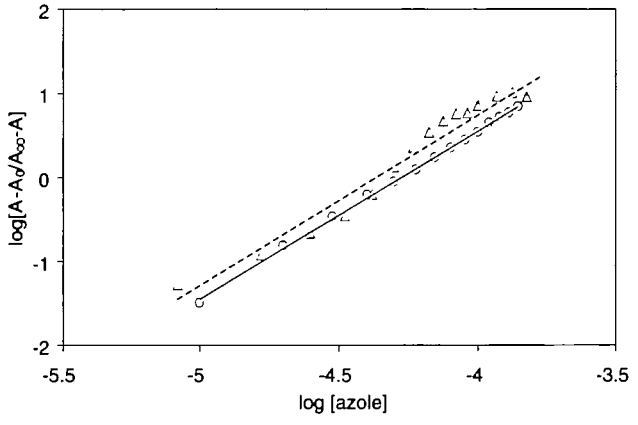


Fig. 3. **Titration of the heme-azole interaction.** Differential spectral titration of azoles with 10 μM heme was performed as described in "MATERIALS AND METHODS," and analyzed by Hill plots. Circles with continuous line, heme-Keto association; triangles with broken line, heme-Mico association.

TABLE II. **The dissociation constants of azoles for heme, the azole concentrations required for half saturation for binding with 10 μM heme (SC50), for the promotion of 50% hemolysis in the presence of 5 μM heme (EC50), and for half inhibition of chloroquine-resistant *P. falciparum* growth (IC50).**

| Azoles | $K_D$ ($M^2$) | $SC_{50}$ (μM)[a,*] | $EC_{50}$ (μM)[a,*] | $IC_{50}$ (μM)[b] |
|---|---|---|---|---|
| Keto | $2.8 \times 10^{-9}$ [a] | 51.2 ± 4.0 | 15.0 ± 1.2 | 3[c] |
| Mico | $1.7 \times 10^{-9}$ [a] | 41.9 ± 0.3 | 4.4 ± 0.7 | 1.5[c] |
| CLT | $2.5 \times 10^{-9}$ [d] | 57.2 ± 12.0 | 3.9 ± 1.2 | 1[e] |

[a]This study. [b]Less than 3% oxygen in the medium. [c]Pfaller MA and Krogstad DJ (*21*). [d]Huy *et al.* (*13*). [e]Saliba and Kirk (*22*). *Calculated from four independent experiments.

TABLE I. **Absorption maxima of ferric proto-heme (ferric protoporphyrin IX) complexed with Keto, Mico, R27, CLT, imidazole, *N*-methylimidazole, or PfHRP2.**

| Sample | Axial ligand | Solvent | Absorption maxima (nm) | | | Reference |
|---|---|---|---|---|---|---|
| Proto-heme | none | Phosphate buffer[a] | 342, 385 | 493 | 613 | This work |
| 〃 | Keto | 〃 | 414 | 534 | 562 | 〃 |
| 〃 | Mico | 〃 | 417 | 534 | 562 | 〃 |
| 〃 | R27 | 〃 | 413 | 533 | 563 | 〃 |
| 〃 | CLT | HEPES[a] | 414 | 534 | 562 | (*13*) |
| 〃 | Imidazole | 40% DMSO[b] | 410 | 535 | 560 | (*13*) |
| 〃 | *N*-Methylimidazole | Phosphate buffer[a] | 413 | 535 | 564 | (*33*) |
| 〃 | PfHRP 2 | Phosphate buffer[c] | 415 | 538 | 566 | (34) |

[a]pH 7.4; [b]HEPES 20 mM, pH 7.4; [c]DMSO content 0.5%; [d]pH 7.6.



Downloaded from http://jb.oxfordjournals.org/ at Islamic Azad University on September 29, 2012

cules (*40*).

*Effect of Azoles on the Heme-R27 Complex*—In previous work (*13*), we have found that CLT can remove heme from the GSH-heme complex to form a stable heme-CLT complex. In this study, we further investigate the effect of Keto and Mico as well as CLT on the PfHRP2-dependent heme detoxification mechanism of malaria. We synthesized the PfHRP2 model peptide R27, the sequence of which comprises the three units of the main repetitive sequence of PfHRP2, Ala-His-His-Ala-His-His-Ala-Ala-Asp. R27 (0.5 mM) in complex with heme (0.5 mM) was studied by ESR spectrometry. The ESR spectrum of the heme-R27 complex (Fig. 4d) revealed the presence of a ferric low-spin with a broad line peak, which is characteristic of ferric heme-peptide complexes (*34, 40*). Thereafter, Keto (0.5 mM) was added to the reaction mixture and the spectrum was recorded again by ESR spectrometry at 4.2 K. The resulting frozen mixture, as shown in Fig. 4e, gave an ESR signal, which is identical to the ESR signal of the heme-Keto complex as already depicted in Fig. 4b. The $g$ values of the heme-peptide complex agree well with those of the heme-azole complexes (Table III), but the line width was characteristically narrowed by the addition of Keto. No further change in the ESR signal was observed by adding excess amounts of Keto (4 mM). These results indicate that the heme-R27 complex can be converted to the heme-Keto complex by the addition of minimal amounts of Keto. Similar ESR spectral changes were also recognized after the addition of Mico and CLT into the heme-R27 complex (Fig. 4, f and g). Therefore, all three azoles might be able to remove heme from the heme-PfHRP2 complex and form heme-azole complexes.

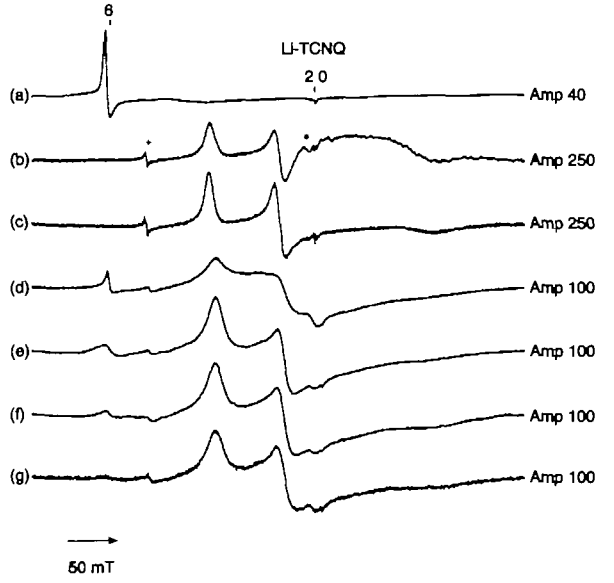


Fig. 4. **ESR spectra of heme-Keto and heme-Mico complexes, and the effect of the azoles on the heme-R27 complex.** ESR spectra of mesoheme (a), heme-Keto complex (b), and heme-Mico complex (c) in DMSO. The spectra of 0.5 mM heme-R27 complex in 100 mM phosphate buffer (pH 7.4) before adding azole (d), and after adding 0.5 mM of Keto (e), Mico (f), or CLT (g). +, weak ESR signal appearing at $g$ = 4.3, which can be assigned to a non-heme type iron complex or impurities; *, ghost cavity. All samples were recorded at 4.2 K.

*Inhibition of GSH-Dependent Heme Degradation by Keto and Mico*—The absorption spectra of the heme-Keto and heme-Mico complexes, like the heme-CLT complex (*13*), did not change following the addition of GSH, indicating that these complexes do not interact with GSH (data not shown). The GSH-dependent degradation of heme (3 μM) in the absence or presence of Keto or Mico (6 μM) was monitored as the decline in the absorbance at 396 nm. The results shown in Fig. 5 indicate that both of Keto and Mico totally inhibit GSH-dependent heme degradation under our experimental conditions.

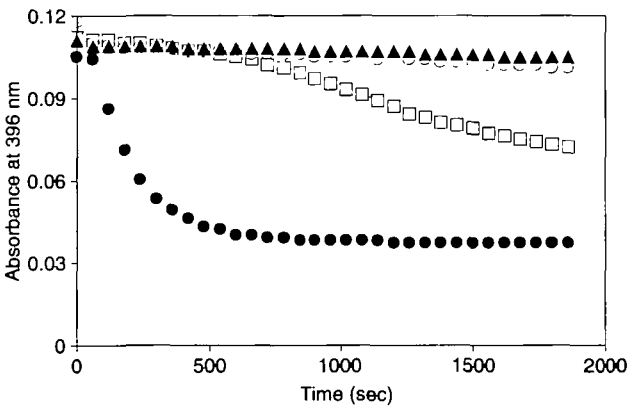


Fig. 5. **Inhibition of GSH-dependent heme degradation by azoles.** GSH-dependent heme degradation was monitored by changes in the absorbance at 396 nm. Heme (3 μM) and GSH (2 mM) were mixed in 0.2 M HEPES buffer (pH 7.4) in the absence (filled circles) or presence of 6 μM Keto (open circles), or 6 μM Mico (triangles). Heme (3 μM) only in the same buffer was also recorded as a control (rectangles).

TABLE III. **The $g$-values and crystal field parameters* of heme-Keto, heme-Mico, and heme-R27 complexes and related ferric low-spin complexes.**

| Sample | $g_1$ | $g_2$ | $g_3$ | $\|R/\mu\|$ | $\|\mu/\lambda\|$ | Reference |
|---|---|---|---|---|---|---|
| $Fe^{3+}$ mesoprotoporphyrin IX-[Keto]$_2$[a] | 1.46 | 2.26 | 2.97 | 0.572 | 3.104 | This work |
| $Fe^{3+}$ mesoprotoporphyrin IX-[Mico]$_2$[a] | 1.49 | 2.26 | 2.98 | 0.554 | 3.254 | 〃 |
| $Fe^{3+}$ mesoprotoporphyrin IX-R27[b] | 1.50 | 2.26 | 2.95 | 0.570 | 3.250 | 〃 |
| $Fe^{3+}$ mesoprotoporphyrin IX-R27 + Keto[b] | 1.46 | 2.26 | 2.97 | 0.572 | 3.104 | 〃 |
| $Fe^{3+}$ mesoprotoporphyrin IX-R27 + Mico[b] | 1.49 | 2.26 | 2.98 | 0.554 | 3.254 | 〃 |
| $Fe^{3+}$ mesoprotoporphyrin IX-R27 + CLT[b] | 1.46 | 2.26 | 2.98 | 0.566 | 3.121 | 〃 |
| $Fe^{3+}$ mesoprotoporphyrin IX-[imidazole]$_2$[b] | 1.48 | 2.24 | 2.98 | 0.536 | 3.316 | (*13*) |
| $Fe^{3+}$ mesoprotoporphyrin IX-[CLT]$_2$[a] | 1.46 | 2.26 | 2.98 | 0.566 | 3.121 | (*13*) |
| Cyt *b*-559 from maize[b] | 1.54 | 2.27 | 2.94 | 0.570 | 3.364 | (*33*) |
| $Fe^{3+}$ protoporphyrinIX-[*N*-methylimidazole]$_2$[b] | 1.52 | 2.26 | 2.95 | 0.560 | 3.342 | (*33*) |
| Clorodeuterohemin dimethyl ester-[imidazole]$_2$[c] | 1.53 | 2.25 | 2.92 | 0.552 | 3.592 | (*38*) |

[a]In DMSO; [b]in phosphate buffer pH 7.4; [c]in chloroform. *Calculated using Bohan's proposal (*41*).



Downloaded from http://jb.oxfordjournals.org/ at Islamic Azad University on September 29, 2012

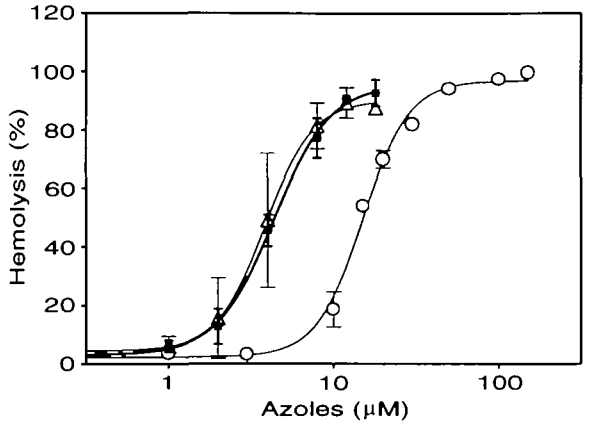


Fig. 6. **Effect of azoles on heme-induced hemolysis.** The extent of hemolysis is expressed as percent. Suspensions of erythrocytes were incubated with 5 μM heme alone or with various concentrations of Keto (open circles), CLT (triangles), or Mico (stars), then shaken at 140 cycles/min for 150 min. Thereafter, the degree of hemolysis was measured as described in "MATERIALS AND METHODS." Points are mean hemolysis (%) ± SE of four independent experiments.

*Concentration of Azoles That Cause 50% Erythrocyte Hemolysis ($EC_{50}$) in the Presence of 5 μM Heme*—The enhancement of heme-induced hemolysis by CLT has been found (*13*). Here, we further investigated the effect of Keto and Mico on heme-induced hemolysis, and determined the concentrations of three azoles that cause 50% erythrocyte hemolysis ($EC_{50}$) in the presence of 5 μM heme. In the control, we found that azoles alone up to 20 μM of CLT and Mico, and up to 150 μM of Keto had no effect on hemolysis in the absence of heme (data not shown). In addition, the hemolysis of less than 5% of erythrocytes was induced by 5 μM heme in the absence of azoles. Upon adding azoles, the extent of hemolysis was significantly increased and depended on the concentration of azoles added (Fig. 6). The dose-response curves for enhancement of azoles on heme-induced hemolysis are sigmoid-shaped. The concentrations of azoles that cause the heme-induced 50% erythrocytes hemolysis ($EC_{50}$) are 15.0 ± 1.2, 3.9 ± 1.2, and 4.4 ± 0.7 μM for Keto, CLT and Mico, respectively, as shown in Table II.

## DISCUSSION

We studied the interactions between heme and two azoles (Keto and Mico) using optical absorption and ESR spectroscopy. The observed optical and ESR spectra of the heme-Keto and heme-Mico complexes were distinctly different from those of heme, demonstrating that both of Keto and Mico interact with heme. Furthermore, the optical and ESR spectra, as well as the parameters of the heme-Keto and heme-Mico complexes (Tables I and III), showed a strikingly resemblance to those of low-spin, six-coordinate, and bis-imidazole ligated species, indicating that they form a six coordinate complex with heme. The six coordinate binding mode has been observed frequently for naturally occurring heme enzymes and synthetic iron-porphyrin complexes (*33, 34*). Furthermore, the crystal field parameters, rhombicity ($|R/\mu|$) and tetragonality ($|\mu/\lambda|$), of the heme-Keto and heme-Mico complexes, calculated in terms of Bohan's proposal (*41*), are in good agreement with those of heme-imidazole complexes (Table III). On the bases of the results obtained from ESR and optical measurements, as well as from crystal field calculation, we conclude that the axial ligands of the heme-Keto and heme-Mico complexes are, therefore, the nitrogenous donors derived from the imidazole groups of the azoles.

Since it has been reported that heme in aqueous-DMSO (40%) exists as a monomer form up to a heme concentration of 26.6 μM (*33–35*), we used a solution containing 40% DMSO to analyze the binding mode of heme and azoles. In 40% DMSO, the analysis of spectral titration in terms of Hill plots indicated that Keto and Mico have an affinity to heme with a $K_D$ of $2.8 \times 10^{-9}$ $M^2$ and $1.7 \times 10^{-9}$ $M^2$, respectively, as shown in Fig. 3 and Table II. Compared to the dissociation constant of the heme-CLT complex ($K_D$ = $2.5 \times 10^{-9}$ $M^2$) (*13*), we suggest that the three azoles have almost the same affinity to heme under these artificial conditions, even though Mico seems to have a little stronger affinity to heme. A comparison of the $SC_{50}$ values of three azoles to 10 μM heme also indicates the same tendency in the affinity for heme as shown in Table II.

In this work, we demonstrate that Keto and Mico behave similarly to CLT in binding to heme in 40% DMSO. In the binding with Keto and Mico, heme assumes a ferric low-spin state (S = 1/2), with two nitrogenous ligands derived from the imidazole moieties of two azole molecules. Furthermore, we reveal that the formation of the heme-Keto and heme-Mico complexes, like the heme-CLT complex (*13*), protects heme from GSH-dependent degradation (Fig. 5), that three of the azoles convert the R27-heme complex to the heme-azole complex (Fig. 4), and the heme-azole complex damages the erythrocyte membrane more seriously than does free heme (Fig. 6). CLT and Mico have a stronger ability to promote heme-induced hemolysis than Keto, despite their similar affinities for heme (Fig. 3 and Table II). This indicates that the promotion of heme-induced hemolysis by azoles might be due to the effect of their structure, although the differences in their affinity for heme can not be excluded because the actual cooperation occurring inside the cells is not known. In view of previous studies (*19–23*), Mico and CLT clearly have higher antimalarial activity than Keto, as indicated by the $IC_{50}$ in Table II. The stronger antimalarial activities of Mico and CLT might arise from their stronger activities to promote heme-induced hemolysis of Mico and CLT than that of Keto (Fig. 6). Based on these results, we suggest that Keto and Mico, like CLT, possess an antimalarial mechanism relating to their inhibition of heme polymerization and of GSH-dependent heme catabolism.

The plasma level of Mico is not high enough to inhibit malarial growth when taken in a 250-mg oral dose (*42*). However, given orally (single dose of 1 g), CLT is absorbed rather well, reaching 2 μM in the plasma within 2–4 h of administration (*43*). The high partition in erythrocyte targets, and the proven clinical safety of CLT after oral administration for one week (*43, 44*) offer promise as a new antimalarial. Keto also can reach 12 μM in serum at an oral dose of 400–600 mg without important side-effects (*45*). These data indicate that azoles given orally could be absorbed and reach the plasma at sufficiently high concentrations to inhibit the growth of malaria.

The antimalarial mechanism of CLT is not well understood, but it has been claimed to have a major impact on



Downloaded from http://jb.oxfordjournals.org/ at Islamic Azad University on September 29, 2012

calcium ion fluxes (*23–26*) and the disturbance of hemoglobin catabolism in the malarial parasite (*13*). In the present study, we suggest that other azoles (Keto and Mico), like CLT, might have an antimalarial mechanism: arising from the inhibition both of heme-polymerization and heme-degradation through the formation of a complex with heme resulting in the disruption of the defense system of malaria against free heme. Furthermore, the decomposition of the membrane triggered by the heme-azole complexes is thought to play an important role in the antimalarial action of azoles.

The authors thank Professor Michael Betenbaugh, Department of Chemical Engineering, The Johns Hopkins University, Baltimore, MD 21218, USA, for critical reading of the manuscript.

## REFERENCES


1. Trigg, P.I. and Kondrachine, A.V. (1998) *Malaria: Parasite Biology, Pathogenesis, and Protection* (Sherman, I.W., ed.) pp. 11–22, Blackwell Science, Oxford, UK
2. Chou, A.C. and Fitch, C.D. (1980) Hemolysis of mouse erythrocytes by ferriprotoporphyrin IX and chloroquine. Chemotherapeutic implications. *J. Clin. Invest.* **66**, 856–858
3. Kirschcner-Zilber, I., Rabizadeh, E., and Shaklai, N. (1982) The interaction of hemin and bilirubin with the human red cell membrane. *Biochim. Biophys. Acta* **690**, 20–30
4. Menting, J.G., Tilley, L., Deady, L.W., Ng, K., Simpson, R.J., Cowman, A.F., and Foley, M. (1997) The antimalarial drug, chloroquine, interacts with lactate dehydrogenase from Plasmodium falciparum. *Mol. Biochem. Parasitol.* **88**, 215–224
5. Ahmad, H., Singh, S.V., and Awasthi, Y.C. (1991) Inhibition of bovine lens glutathione S-transferases by hematin, bilirubin, and bromosulfophthalein. *Lens Eye Toxic Res.* **8**, 431–440
6. Wellems, T.E. and Howard, R.J. (1986) Homologous genes encode two distinct histidine-rich proteins in a cloned isolate of *Plasmodium falciparum*. *Proc. Natl. Acad. Sci. USA* **83**, 6065–6069
7. Sullivan, J.D.J., Gluzman, I.Y., and Goldberg, D.E. (1996) *Plasmodium* hemozoin formation mediated by histidine-rich proteins. *Science* **271**, 219–222
8. Cannon, J.B., Kuo, F., Pasternack, R.F., Wong, N.M., and Muller-Eberhard, U. (1984) Kinetics of the interaction of hemin liposomes with heme binding proteins. *Biochemistry* **23**, 3715–3721
9. Rose, M.Y., Thompson, R.A., Light, R.W., and Olson, J.S. (1985) Heme transfer between phospholipid membranes and uptake by apohemoglobin. *J. Biol. Chem.* **260**, 6632–6640
10. Ginsburg, H. and Demel, R.A. (1983) The effect of ferriprotoporphyrin IX and chloroquine on phospholipid monolayers and the possible implications to antimalarial activity. *Biochim. Biophys. Acta* **732**, 316–319
11. Ginsburg, H. and Demel, R.A. (1984) Interactions of hemin, antimalarial drugs and hemin-antimalarial complexes with phospholipid monolayers. *Chem. Phys. Lipids* **35**, 331–347
12. Atamna, H. and Ginsburg, H. (1995) Heme degradation in the presence of glutathione. A proposed mechanism to account for the high levels of non-heme iron found in the membranes of hemoglobinopathic red blood cells. *J. Biol. Chem.* **270**, 24876–24883
13. Huy, N.T., Kamei, K., Yamamoto, T., Kondo, Y., Kanaori, K., Takano, R., Tajima, K., and Hara, S. (2002) Clotrimazole binds to heme and enhances heme-dependent hemolysis: Proposed antimalarial mechanism of clotrimazole. *J. Biol. Chem.* **277**, 4152–4158
14. Shviro, Y. and Shaklai, N. (1987) Glutathione as a scavenger of free hemin. A mechanism of preventing red cell membrane damage. *Biochem. Pharm.* **36**, 3801–3807
15. Atamna, H. and Ginsburg, H. (1997) The malaria parasite supplies glutathione to its host cell—investigation of glutathione transport and metabolism in human erythrocytes infected with *Plasmodium falciparum*. *Eur. J. Biochem.* **250**, 670–679
16. Luersen, K., Walter, R.D., and Muller, S. (2000) *Plasmodium falciparum*-infected red blood cells depend on a functional glutathione de novo synthesis attributable to an enhanced loss of glutathione. *Biochem. J.* **346**, 545–552
17. Ginsburg, H. (1999) An intergrated model of chloroquine action. *Parasitology Today* **15**, 357–360
18. Ginsburg, H., Famin, O., Zhang, J., and Krugliak, M. (1998) Inhibition of glutathione-dependent degradation of heme by chloroquine and amodiaquine as a possible basis for their antimalarial mode of action. *Biochem. Pharm.* **56**, 1305–1313
19. Pfaller, M.A. and Krogstad, D J. (1981) Imidazole and polyene activity against chloroquine-resistant *Plasmodium falciparum*. *J. Infect. Dis.* **144**, 372–375
20. Pfaller, M.A., Segal, J.J., and Krogstad, D.J. (1982) Activity of ketoconazole and its deacyl derivative against *Plasmodium falciparum* and *Candida* isolates. *Antimicrob Agents Chemother.* **22**, 917–922
21. Pfaller, M.A. and Krogstad, D.J. (1983) Oxygen enhances the antimalarial activity of the imidazoles. *Am. J. Trop. Med. Hyg.* **32**, 660–532
22. Saliba, K.J. and Kirk, K. (1998) Clotrimazole inhibits the growth of *Plasmodium falciparum* in vitro. *Trans. R. Soc. Trop. Med. Hyg.* **92**, 666–667
23. Tiffert, T., Ginsburg, H., Krugliak, M., Elford, C., and Lew, V.L. (2000) Potent antimalarial activity of clotrimazole in in vitro cultures of *Plasmodium falciparum*. *Proc. Natl. Acad. Sci. USA* **97**, 331–336
24. Benzaquen, L.R., Brugnara, C., Byers, H.R., Gattoni-Celli, S., and Halperin, J.A. (1995) Clotrimazole inhibits cell proliferation in vitro and in vivo. *Nat. Med.* **1**, 534–540
25. Tiffert, T., Staines, H.M., Ellory, J.C., and Lew, V.L. (2000) Functional state of the plasma membrane $Ca^{2+}$ pump in *Plasmodium falciparum*-infected human red blood cells. *J. Physiol.* **525**, 125–134
26. Aktas, H., Fluckiger, R., Acosta, J.A., Salvage, J.M., Palakurthi, S.S., and Halperin, J.A. (1998) Depletion of intracellular $Ca^{2+}$ stores, phosphorylation of eIF2$\alpha$, and sustained inhibition of translation initiation mediate the anticancer effects of clotrimazole. *Proc. Natl. Acad. Sci. USA* **95**, 8280–8285
27. Shaklai, N., Shviro, Y., Rabizadeh, E., and Kirschner-Zilber, I. (1985) Accumulation and drainage of hemin in the red cell membrane. *Biochim. Biophys. Acta* **821**, 355–366
28. Van Holde, K.E. (1971) *Physical Biochemistry*, pp. 62–64, Prentice Hall, Englewood Cliffs, NJ
29. Brault, D. and Rougee, M. (1974) Binding of imidazole and 2-methylimidazole by hemes in organic solvents. Evidence for five-coordination. *Biochem. Biophys Res Commun.* **57**, 654–659
30. Sahini, V.E., Dumitrescu, M., Volanschi, E., Birla, L., and Diaconu, C. (1996) Spectral and interferometrical study of the interaction of haemin with glutathione. *Biophys. Chem.* **58**, 245–253
31. Kaminsky, L.S., Byrne, M., and Davison, A.J. (1972) Iron ligands in different forms of ferricytochrome c: the 620-nm band as a probe. *Arch. Biochem. Biophys.* **150**, 355–361
32. Pasternack, R.F., Gillies, B.S., and Stahlbush, J.R. (1978) Kinetics and thermodynamics of the reactions of two iron (III) porphyrins with imidazole and 1-methylimidazole in dimethyl sulfoxide. *J. Am. Chem. Soc.* **100**, 2613–2619
33. Babcock, G.T., Widger, W.R., Cramer, W.A., Oerling, W.A., and Metz, J.G. (1985) Axial ligands of chloroplast cytochrome b-559: identification and requirement for a heme-cross-linked polypeptide structure. *Biochemistry* **24**, 3638–3645
34. Choi, C.Y.H., Cerda, J.F., Chu, H.A., Babcock, G.T., and Marletta, M.A. (1999) Spectroscopic characterization of the heme-binding sites in *Plasmodium falciparum* histidine-rich protein 2. *Biochemistry* **38**, 16916–16924
35. Beaven, G.H., Chen, S., D'Albis, A., and Gratm, W.B. (1974) A spectroscopic study of the haemin--human-serum-albumin system. *Eur. J. Biochem.* **41**, 539–546




Downloaded from http://jb.oxfordjournals.org/ at Islamic Azad University on September 29, 2012

36. Collier, G.S., Pratt, J.M., De Wet, R., and Tshabalala, C.F. (1979) Studies on haemin in dimethyl sulphoxide/water mixtures. *Biochem. J.* **179**, 281–289
37. Egan, T.J., Mavuso, W.W., Ross, D.C., and Marques, H.M. (1997) Thermodynamic factors controlling the interaction of quinoline antimalarial drugs with ferriprotoporphyrin IX. *J. Inorg. Chem.* **68**, 137–145
38. Momenteau, M. (1973) The physical chemistry of hemes and hemopeptides. I. Physiochemical properties and reduction of chlorodeuterohemin in organic solvent. *Biochim. Biophys. Acta* **304**, 814–827
39. Tajima, K. (1989) A possible model of a hemoprotein-hydrogen peroxide complex. *Inorg. Chim. Acta* **163**, 115–122
40. More, C., Belle, V., Asso, M., Fournel, A., Roger, G., Guigliarelli, B., and Bertrand, P. (1999) EPR spectrocopy: A powerful technique for the structural and functional investigation of metalloproteins, *Biospectroscopy* **5**, S3–S18
41. Bohan, T.L. (1977) Analysis of low-spin ESR spectra of ferric heme proteins: a reexamination. *J. Magn. Reson.* **26**, 109–118
42. Kobylinska, M., Kobylinska, K., and Sobik, B. (1996) High-performance liquid chromatographic analysis for the determination of miconazole in human plasma using solid-phase extraction. *J. Chromatogr. B.* **685**, 191–195
43. Brugnara, C., Armsby, C.C., Sakamoto, M., Rifai, N., Alper, S.L., and Platt, O. (1995) Oral administration of clotrimazole and blockade of human erythrocyte $Ca^{2+}$-activated $K^+$ channel: the imidazole ring is not required for inhibitory activity *J. Pharmacol. Exp. Ther.* **273**, 266–272
44. Brugnara, C., Gee, B., Armsby, C.C., Kurth, S., Sakamoto, M., Rifai, N., Alper, L., and Platt, O.S. (1996) Therapy with oral clotrimazole induces inhibition of the Gardos channel and reduction of erythrocyte dehydration in patients with sickle cell disease. *J. Clin. Invest.* **97**, 1227–1234
45. Graybill, J.R., Lundberg, D., Donovan, W., Levine, H. B., Rodriguez, M.D., and Drutz, D.J. (1980) Treatment of coccidioidomycosis with ketoconazole: clinical and laboratory studies of 18 patients. *Rev. Infect. Dis.* **2**, 661–673

Downloaded from http://jb.oxfordjournals.org/ at Islamic Azad University on September 29, 2012